Pyrene Photochemistry in Solid *n*-Alkane Matrices: Comparisons with Liquid-Phase Reactions

Oscar E. Zimerman and Richard G. Weiss*

Department of Chemistry, Georgetown University, Washington, D.C. 20057-1227

Received: July 12, 1999; In Final Form: October 5, 1999

The photochemically induced attachment of pyrene to a series of *n*-alkanes (C*n*, where $n = 8$, 19, 20, 21, 24, and 28), cyclohexane (CyH), and 1-eicosene (C=20) has been investigated as a function of solvent phase, pyrene concentration, radiation wavelength (especially below and above 300 nm), and alkane chain length. Qualitatively, the efficiency and selectivity of attachment are much greater in the solid than in the liquid phases of the alkanes. Efficiency is decreased significantly when the concentration of pyrene in the solid phases is increased above ca. 10^{-5} M. The solid-state reactions are very selective when $n \geq 21$ and the irradiation wavelength is > 300 nm. Under these conditions, only one photoattachment product, a 1-alkylpyrene, can be detected in each case. Mechanistic models consistent with these observations are advanced. They explain the changes in selectivity and efficiency based on the location of the pyrene molecules in the solid phase matrices and on the energy available to the highly excited states of pyrene which initiate the attachment processes. The procedures outlined provide a one-step recipe for the syntheses of some rather difficult to obtain photophysical probes.

Introduction

Despite the widespread perception that pyrene (PyH) is inert to UV/vis radiation, several reports in the literature have demonstrated that it can be attached to a variety of hydrocarbon solvents.[1−4] Previously, we found that PyH can be covalently attached to interior sites of polyethylene (PE) films upon irradiation even at >300 nm (<4.1 eV).[5] Since a large dopant molecule like PyH can reside only in the amorphous and interfacial regions of PE matrices,[6] we asked (1) Would pyrene react if imbedded in the *lamellar crystalline* regions of the polymer? (2) If it were to react in such an environment, what would be the preferred position on pyrene of substitution/addition? and (3) What would be the preferred position of substitution among the various types of C−H bonds of the alkyl chains?

A reasonable model for the lamellar microcrystallites of PE is the solid phases of long *n*-alkanes. Here, we compare results from irradiations of PyH in the solid phases of several *n*-alkanes (octacosane (C28: $H(CH_2)_{28}H$), tetracosane (C24: $H(CH_2)_{24}H$), heneicosane (C21: $H(CH_2)_{21}H$), eicosane (C20: $H(CH_2)_{20}H$), nonadecane (C19: $H(CH_2)_{19}H$), and octane (C8: $H(CH_2)_8H$)), a cycloalkane (cyclohexane (CyH: $(CH_2)_6$)), and a long alkene (1-eicosene (C=20: $H(CH_2)_{18}CH{=}CH_2$)) with those from the corresponding liquid phases. Irradiations in the lower temperature solid morph of C21,[7] phase II, were most interesting since they led to "clean" reactions and very high chemical yields of 1-heneicosylpyrene. Under the same irradiation conditions, almost no reaction was detected in liquid C21 or the other liquid alkanes. Multiple photoproducts were observed in the higher temperature solid morph of C21, phase I or "rotator" phase,[7] and the solid phases of the other solvents. However, the major photoproducts appear to be 1-alkylpyrenes. We provide a rationalization for these surprising results and note the potential synthetic utility of these photoreactions: a wide variety of 1-alkylpyrenes can be synthesized in one facile step. In fact, we find evidence for no more than one photoproduct between pyrene and solid C24 or C28, despite the presence of perceptible amounts of impurities in the neat solvents.

* Corresponding author phone, (202) 687-6013; fax, (202) 687−6209; e-mail, weissr@gusun.georgetown.edu.

Experimental Section

Reagents. Pyrene (PyH; Aldrich 99%) was recrystallized three times from 96% ethanol, chromatographed on an alumina column using benzene as eluant, and sublimed under vacuum (mp 148−149 °C (lit.[8] mp 149−151 °C)). 1-Ethylpyrene (C2Py) (mp 95−96 °C (lit.[9] mp 94−95 °C)), 1-octylpyrene (C8Py), 1-hexadecylpyrene (C16Py), and 1,3-di(1-pyrenyl)propane (Py3Py) (mp 148−149 °C (lit.[10] mp 148−150 °C)) were obtained from Molecular Probes and used without further purification. 1,22-Di(1-pyrenyl)docosane (Py22Py) was a gift from Dr. Klaas Zachariasse of the Max Planck Institut für Biophysikalische Chemie, Göttingen. Gel permeation chromatographic analyses were performed on a Hewlett-Packard Series 1100 ChemStation equipped with a diode array detector (4 nm bandwidth), and a Polymer Laboratories PLgel (3 μm MIXED-E; 300 mm length × 7.5 mm ID) column with tetrahydrofuran (THF; Fisher Scientific, HPLC grade) as eluant; PyH, C2Py, C8Py, C16Py, and Py3Py were > 99%, and Py22Py was > 96% pure. CyH (Fisher Scientific) was vigorously stirred with H_2SO_4 at room temperature for 8 days in the dark, decanted, washed several times with 25% aqueous NaOH, passed over a 5 cm length × 4 cm Al_2O_3 column, distilled, and stored in the dark over 4 Å molecular sieves under an N_2 atmosphere.[11] Methanol (Mallinckrodt UltimAR 99.9%), acetonitrile (Fisher Scientific, HPLC grade), *n*-hexane (EM-Science, Spectrophotometric grade), *n*-pentane (Fisher Scientific, IR certified), and dichloromethane (Mallinckrodt, spectrophotometric grade) were used as received. C8 (Aldrich, 99 + %), and C=20 (TCI America, mp 27−29 °C (lit.[12] mp 28.6 °C)) were used as received. C19 (mp 32−33 °C (lit.[13] mp 32.0 °C)), C20 (mp

10.1021/jp992339h CCC: $18.00
Published on Web 11/12/1999

36−37 °C (lit.[13] mp 36.6 °C)), and C21 (mp 40−41 °C (lit.[14] mp 40.14 °C)) were obtained from Humphrey Chemicals Co. and were recrystallized three times from 95:5 acetone/hexane.[15] C24 (mp 51−52 °C (lit.[12] mp 50.9 °C)) and C28 (mp 62−63 °C (lit.[12] mp 61.4 °C)), also from Humphrey, were recrystallized three times from toluene and passed over a 5 cm length × 4 cm Al_2O_3 column using hexane as eluant.[13,15]

Sample Preparations: PyH and C2Py in Hydrocarbon Matrices. A mixture of a small amount of PyH (or C2Py) and a hydrocarbon solvent was melted and gently shaken in a vial. The precise concentration was calculated in the isotropic phase with a 1 mm path-length quartz cell using Beer's law and assuming ϵ_{336} 55 550 M^{-1} cm^{-1} for PyH[16] and ϵ_{343} 39 800 M^{-1} cm^{-1} for C2Py.[17] An aliquot of appropriate composition was transferred to a flattened glass capillary (8 mm (i.d.) × 0.8 mm (i.d.) × 30 mm; transmittance cutoff 300 nm; VitroCom) and sealed after being degassed by four freeze−pump−thaw cycles at < 10^{-5} Torr on a mercury-free vacuum line.

UV Irradiations of PyH Samples. Two flattened glass capillaries containing PyH in degassed solvent were heated to the isotropic phase and gently shaken. One was quickly immersed in an ice bath and the other was allowed to cool in the air to room temperature. The samples were irradiated by the output from a 450 W Hanovia medium-pressure Hg arc lamp in baths that maintained specific temperatures/phases: solid phases of CyH, C19, C20, and C=20 in ice−water; solid phase of C8 in dry ice/ethanol;[18] liquid phase of CyH, phase II of C21, and solid phases of C24 and C28 in water at room temperature; phase I of C21 in a water bath at 35 ± 0.3 °C; liquid phase of C=20 in a water bath at ca. 45 °C; liquid phases of other alkanes in a water bath at ca. 50 °C. Irradiation times were 1 h unless indicated otherwise. In addition, samples in solid C21 and CyH were irradiated at room temperature and ca. 0 °C respectively with an Ultra Violet Products low-pressure Hg arc lamp (254 nm) for various periods, using methanol as a filter to remove 185 nm radiation.

After being irradiated, the solid samples were heated to their isotropic phases, shaken, and cooled. Relevant spectra were recorded. Then, each sample was melted and dissolved in about an equal volume of THF for further analyses.

Instrumentation. UV/vis absorption spectra were recorded on a Perkin-Elmer Lambda-6 spectrophotometer. Excitation (corrected for detector response) and emission spectra (uncorrected) were obtained on a Spex Fluorolog 111 spectrofluorimeter (linked to a PC) with a 150 W high-pressure xenon lamp and 0.25 mm slits (ca. 0.9 nm resolution) on both the excitation and the emission monochromators. Samples were thermostated (±0.3 °C) using a VWR 1140 circulating constant temperature bath. Fluorescence rise and decay histograms were obtained with an Edinburgh Analytical Instruments model FL900 single photon counting system using H_2 as the lamp gas. Samples in capillaries were immersed in a quartz cuvette containing *n*-hexadecane and aligned at ca. 45° to the incident radiation. The emission was detected at a right angle from the back face of the sample. An "instrument response function" was determined using Ludox as scatterer and without polarizers. Data were collected in 1023 channels (0.504 or 1.009 ns/channel), and 10^4 counts were collected in the peak channel unless indicated otherwise. Proton NMR spectra were recorded on a Mercury 300 MHz Varian spectrometer interfaced to a Sun SparcStation 5.

Gas chromatograms were obtained with a Hewlett-Packard 5890A gas chromatograph equipped with a flame ionization detector and a capillary column (Alltech DB-5 Durabond FSOT cross linked 5% phenyl methyl silicone; 15 m × 0.25 m × 0.25 μm) and a Hewlett-Packard 3393A integrator. GC-MS was performed with a Fisons MD 800 GC-MS with the same analytical column.

Fluorescence Decay Data Treatment. Curve fitting and deconvolution employed nonlinear least-squares routines with software supplied by Edinburgh Instruments. A range from time = 0 (a channel before the onset of the instrument response signal) to at least two decades of decay from the peak channel were included in the analyses. Goodness of fit was assessed from χ^2 values and plots of residuals. Data were analyzed using exponential, distribution, and global analysis methods.[19] The exponential method was used when a single wavelength of emission and excitation was employed or no correlations were made among the decays. Several wavelengths were analyzed for each of the data sets; scatter components (always present) were included as unlinked decays.

Results and Discussion

Historical and Mechanistic Considerations. Irradiation of pyrene and other polycyclic aromatic hydrocarbons (PAHs) in paraffinic solvents has been studied for many years and still attracts much attention.[20] Initially, isolated PAH molecules in solid solutions were thought to be inert to UV/vis irradiations. However, the Bordeaux group, especially, has demonstrated that many PAHs (including triphenylene,[21] phenanthrene,[22] and anthracene[23]) can undergo relatively efficient photoreactions with *n*-alkanes at low temperatures. The radicals produced lead to solvent addition (ArH_2R) and/or substitution products (ArR).[21] Quantum yields for the overall processes with pyrene are ~10^{-4} to 10^{-6}, depending on the wavelength and flux of photons.[21] In addition, irradiation of PyH in very polar, protic media is known to produce at least two photoproducts.[24,25]

However, there has been no study of the photochemistry of pyrene in a series of alkanes which (1) allows the selectivity of pyrenyl substitution for hydrogen at several different C−H bonds to be probed, (2) compares the influence of several phases of one *n*-alkane on the efficiency and type of photoreaction, and (3) employs relatively low energy radiation (>300 nm; < 4.1 eV) to initiate the photochemistry. These are the major focus of this work.

Since the vertical ionization potential of pyrene is ca. 6.2 eV,[26] excitation at 185 nm (6.7 eV)[3] produces highly excited singlet states (i.e., S_n**, "high-Rydberg" states with principal quantum numbers ≥ 10).[27] When λ_{ex} > 240 nm (<5.1 eV), initial excitation by one photon and intersystem crossing leads to a longer-lived triplet state (T_1). It can be excited to a very high triplet (T_n**) by absorption of a second photon. Energy transfer to a dissociative state of a solvent molecule, RH, competes with rapid internal conversion to S_1 or T_1. Thus, highly excited states of pyrene initiate the photochemistry by transferring energy to neighboring solvent molecules; pyrene S_n** or T_n** states are sensitizers for excitation and scission of a C−H "chromophore". In both cases, the subsequent steps involve addition of radicals (or radical-ions), such as $H^\bullet$ or $R^\bullet$, to (presumably) *ground-state* pyrene in a solvent cage. A simplified mechanism of the probable events is shown in Scheme 1. If diffusion of either the pyrene or radical (or its precursor) from the solvent cage is more rapid than addition, no photochemistry involving pyrene will be observed. Clearly, molecular containment in a solvent cage[28] is a necessary feature of the mechanism outlined in Scheme 1. It also suggests that the nature of the photochemical events from the two-photon mechanism may be wavelength dependent.

Ground-state pyrene is most easily attacked by radicals and cations at the 1-position,[29] and ab initio calculations indicate it

SCHEME 1

$$\mathrm{PyH} \xrightarrow[185\ \mathrm{nm}]{h\nu} {}^1\mathrm{PyH}^{**} \quad (1)$$

$$\mathrm{PyH} \xrightarrow[254\ \mathrm{or}\ >300\ \mathrm{nm}]{h\nu} {}^1\mathrm{PyH}^{*} \quad (2)$$

$${}^1\mathrm{PyH}^{*} \xrightarrow{\mathrm{ISC}} {}^3\mathrm{PyH}^{*} \quad (3)$$

$${}^3\mathrm{PyH}^{*} \xrightarrow{h\nu} {}^3\mathrm{PyH}^{**} \quad (4)$$

$$\mathrm{R\text{-}H} + (1\ \mathrm{or}\ 3)\mathrm{PyH}^{**} \longrightarrow \mathrm{R\text{-}H}^{**} + \mathrm{PyH} \quad (5)$$

$$\mathrm{R\text{-}H}^{**} \longrightarrow \mathrm{R}^{\cdot} + \mathrm{H}^{\cdot} \quad (6)$$

$$\mathrm{R}^{\cdot} + \mathrm{PyH} \longrightarrow \mathrm{R\text{-}Py\text{-}H}^{\cdot} \quad (7)$$

$$\mathrm{H}^{\cdot} + \mathrm{PyH} \longrightarrow \mathrm{H\text{-}Py\text{-}H}^{\cdot} \xrightarrow{[\mathrm{H}^{\cdot}]} \mathrm{PyH_3} \quad (8)$$

$$\mathrm{R\text{-}Py\text{-}H}^{\cdot} \longrightarrow \mathrm{PyR} + \mathrm{H}^{\cdot} \quad (9)$$

$$\mathrm{R\text{-}Py\text{-}H}^{\cdot} \xrightarrow{[\mathrm{H}^{\cdot}]} \mathrm{R\text{-}PyH_2} \quad (10)$$

TABLE 1: Melting Temperatures (T_{melt}) and Rotator Crystal Transition Temperatures (T_{rx}) for the Hydrocarbon Solvents Employed

	name	formula	T_{melt} (°C)	T_{rx} (°C)	cell symmetry[a]
CyH	cyclohexane	C_6H_{12}	6.7[43]	−87[43,44]	
C8	*n*-octane	C_8H_{18}	−56.4[38]	-	T
C19	*n*-nonadecane	$C_{19}H_{40}$	32.5[38]	22.8[38]	O ⊥
C20	*n*-eicosane	$C_{20}H_{42}$	36.5[38]	36.2[38]	T
C=20	1-eicosene	$C_{20}H_{40}$	28.0[42]	26.5[42]	O ⊥[42]
C21	*n*-heneicosane	$C_{21}H_{44}$	40.5[38]	32.5[38]	O ⊥, H⊥
C24	*n*-tetracosane	$C_{24}H_{50}$	51.5[38]	48.1[38]	T
C28	*n*-octacosane	$C_{28}H_{58}$	62.5[38]	58.0[38]	O ⊥

[a] Phase in which irradiations were conducted: T = triclinic; O = orthorhombic; H = hexagonal (rotator); ⊥ = perpendicular.

to be the most reactive site of the first excited-singlet state, also.[30] Based on comparative analyses of emission spectra, 1-methylpyrene was indicated as the major photoproduct from irradiation of pyrene in solid methane.[2] The photochemistry of PyH has also been investigated in solid and liquid cyclohexane and methylcyclohexane using <300 nm radiation.[2−4,31] The photoproduct distributions differ with 185 nm (presumably one-photon excitation) and 254 nm (4.9 eV; presumably two-photon excitation).[32] Photoproducts from substitution/addition at the 1- and 4-positions were inferred based on mass spectral analyses.[4] Irradiation (>300 nm) of PyH in polyethylene films leads to at least two distinct species whose fluorescence spectra are very dependent on the wavelength of excitation (λ_{ex}).[33]

Description of Solid Phases. In Table 1 is listed the melting (T_{melt}) and solid−solid transition temperatures (T_{rx})[34] of the hydrocarbon matrices employed. In general, individual *n*-alkane molecules in their crystalline lattices are in fully extended (all-transoid) conformations and are packed side-by-side in layers.[7,14,35] The long molecular axes are either perpendicular to the layer (as in orthorhombic packing[7]) or tilted (as in triclinic packing with long-range, herringbone patterns of layers[36,37]). The crystalline phase of C8 is triclinic.[38,39] The lower temperature solid phases of C19 and C21 are orthorhombic.[40,41a] Their higher temperature solids are hexagonal rotator phases[41a] in which there is significant rotational freedom about long molecular axes.[7,14,41] The unit cells of the lower temperature crystalline phases of C20, C24, and C28 are triclinic,[41b] and these molecules display one or more hexagonal rotator phases, also.[14,41b]

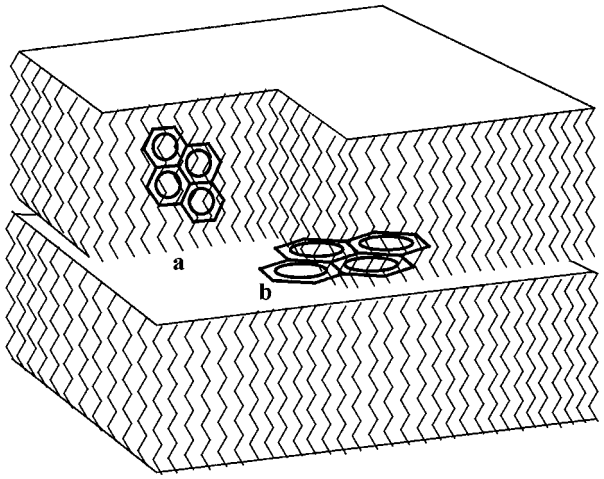

Figure 1. Cartoon representation of possible solubilization sites of pyrene molecules in an *n*-alkane solid matrix.

C=20 was employed as a matrix to explore the influence of an unsaturated group near a layer interface on the photochemistry of PyH. Unlike C20, the lower temperature crystalline phase of C=20 is orthorhombic; it also forms a hexagonal rotator phase.[42]

Between its melting temperature, 6.7 °C,[43] and its transition to a highly ordered crystalline phase at −87 °C,[43,44] CyH exists in a plastic phase[43] where individual molecules maintain their position in the lattice but tumble relatively rapidly.

Potential Sites for PyH Molecules in Solid Hydrocarbon Matrices; Comparisons with Sites in PE. The solid phases of the *n*-alkanes can accommodate pyrene molecules in several site types. The one(s) favored depends on several factors. Some are related to the length of a specific *n*-alkane (i.e., how closely can a pyrene molecule be substituted isomorphously for *n* molecules of alkane within a layer), and others are generic to how *n*-alkanes pack. Regardless, the "stiffness" of the walls[28] of all of the potential sites makes it unlikely that PyH molecules can reorient during their excited-state lifetimes; where they reside in their ground states is where they will react.

One possible site, within an *n*-alkane layer (Figure 1, site **a**), is analogous to the *interiors* of lamellar microcrystallites of PE. As mentioned, guest molecules such as pyrene do not enter PE microcrystallites but remain in the amorphous and interfacial regions.[45,33,46] They may be forced to reside within lamellae of *n*-alkane solid phases since there is no amorphous alternative. If the length or breadth of a pyrene molecule (10.0 Å or 9.2 Å, respectively[47]) is near the thickness of an *n*-alkane layer, quasi-isomorphous substitution may be possible. Furthermore, the average angle between the long axis of a pyrene molecule and the direction of extension of polymethylene chains on the *surface* of a PE microcrystallite (i.e., an interfacial site in polyethylene) is ca. 35°.[48] A similar angle may be preferred for pyrene molecules if *within n*-alkane crystals, but we have no evidence to support this suggestion. Isomorphous substitution, in which one pyrene molecule spans a layer, seems most probable in matrices of solid C8 (layer thickness = 11.02 Å).[49] However, two molecules of pyrene, end-on-end, may be able to replace several molecules within the solid matrices of C19 and longer *n*-alkanes. Since several carbon atoms along a chain would be in contact with pyrene in this scenario, photoproducts with pyrene attached to several different positions of an alkane chain are expected. In fact, even if only C-1 of PyH molecules residing

within the crystalline layers of C8 is able to react, four positional 1-alkylpyrene isomers (from attachment of 1-pyrenyl to the different carbon atoms of octane) are possible.

Alternatively, pyrene molecules may reside *between n*-alkane layers (site **b)**. Such sites have no direct analogy in PE. They would be similar to interfacial regions along the (001) plane of PE microcrystallites[50] if two of them were in face-to-face contact. Since this site type places pyrene molecules in the proximity of the terminal (methyl) carbon atoms of the *n*-alkanes, photoattachment to positions near a chain terminus should be favored. The added thickness of a pyrene molecule (ca. 3.5 Å[47]) when between layers will cause significant disturbances to packing of *n*-alkanes in the vicinity. As a consequence, carbon atoms at C-2 and C-3 may be very near the pyrene ring, also. The effect of placing a pyrene molecule between layers should be comparable to mixing two *n*-alkanes of different lengths. X-ray diffractograms of these solid phases indicate that the terminal methyl and methylene groups for some of the longer chains kink.[7,51]

Regardless of which mode of incorporation is adopted, interactions between pyrene and the vinyl groups of C=20 molecules are possible. The theoretical consequences of this additional interaction are unknown, but it may open a new channel for the photochemistry. For instance, 1,3-cyclohexadiene is known to form a $[2\pi + 2\pi]$ cycloadduct with the triplet state of pyrene ($^3PyH^*$ in Scheme 1).[52]

Sites occupied by PyH in plastic and solid CyH are more difficult to characterize. Even if pyrene is accepted nearly "isomorphously" into the cyclohexane matrices, various types of disturbed domains may be created nearby.[53] In any case, we expect that the occupied sites are very different from those in the solid phases of rod-shaped solvent molecules.

Spectroscopic Measurements of PyH in Liquid and Solid Hydrocarbon Media. The emission spectra (λ_{ex} 343 nm) of ca. 5×10^{-6} M PyH in degassed C21 at room temperature (rapidly cooled solid phase II) and at 47 °C (liquid phase), are presented in Figures 2a and 2b, respectively. In the liquid phase, the emission is like that of unassociated pyrene molecules in other alkane solvents.[54] In the solid phase, excimeric emission dominates the spectrum even though the PyH concentration is well below that expected for excited complexes to form dynamically;[55] the spectrum of the slowly cooled solid sample was like that of Figure 2a.

Others have found evidence for association of PAHs at concentrations where it is not expected. For instance, irradiation at 310 nm of 5×10^{-2} M naphthalene in 1:1 pentane−isopentane at 4.7 Gpa pressure and −15 °C leads to weakly bound dimers which decompose when heated or when the sample is returned to one atmosphere pressure.[56] Also, the formation of PyH microcrystals has been observed far below the concentration for monolayer coverage on silica surfaces.[57] Even at 0.2% coverage, neither the monomeric nor excimeric emissions exhibited a single exponential decay; pyrene molecules form very weakly bound ground-state bimolecular complexes at specific surface sites.[57,58]

The emission and absorption spectra of ca. 5×10^{-6} M PyH in the isotropic phases of all of the hydrocarbon solvents employed match those in liquid *n*-hexane. Emission spectra in the corresponding solid phases exhibit a broad, excimer-like band, centered at 470 nm, which disappears when a sample is liquified. PyH forms "normal" solutions in the isotropic phases ($T > T_{melt}$) and somewhat segregated mixtures in the solids ($T < T_{melt}$).

The ratio of monomeric to excimeric emission intensity in the solid phases varies widely depending on the nature of the alkane matrix. For instance, the emission spectra of neither 10^{-5} M PyH in C=20 nor 10^{-4} M PyH in CyH have a prominent excimer-like band even though the PyH concentrations are 2−20 times higher than that of the sample in Figure 2a. Despite this, there must be some ground-state aggregation in plastic CyH[59] since its emission spectra are excitation wavelength dependent, and it is difficult to envision more than one solubilization site type. A significant fraction of the pyrene molecules must be in electronic contact with others, but they are neither in orientations that approximate an excimer nor are they able to move to such positions during their excited singlet lifetimes. The cause of the dependence of emission spectra from the solid C=20 sample on excitation wavelength is not as clear. Interactions of some of the pyrene molecules with terminal vinyl groups may be a contributing factor.

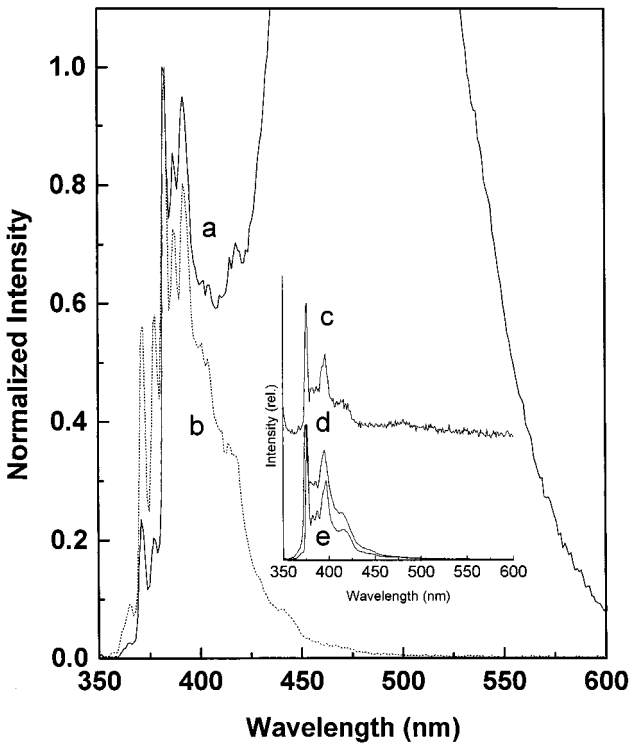

Figure 2. Emission spectra (λ_{ex} 343 nm) of ca. 5×10^{-6} M PyH in degassed C21 (a) at room temperature and (b) at 45 °C. The inset shows emission spectra at 45 °C of (c) isolated C21Py (see text) in hexane at room temperature, (d) ca. 5×10^{-6} M PyH after irradiation for 1 h in degassed solid phase II C21 (room temperature), and (e) unirradiated ca. 10^{-5} M C2Py in C21 at 45 °C. Intensities in (a) and (b) are normalized at 382 nm.

Irradiations of PyH in CyH. Consistent with prior results from irradiations at 189 and 254 nm,[2] at least three products (whose absorption spectra are like that of a pyrenyl or other PAH group) were detected when 10^{-2} or 10^{-4} M PyH was irradiated in liquid (ca. 20 °C) and plastic CyH (ca. 0 °C) at 254 nm and > 300 nm (Figure 3a−c). Qualitatively, photoreaction is much less efficient in the liquid (at room temperature) than in the solid phase, and the photoproduct distributions are similar, but not the same. The higher chemical yields for photoreactions of PyH in liquid CyH reported by others[3,4,21−23] are probably due to a combination of higher energy radiation, higher photon fluxes, and longer irradiation times than employed here.

Regardless, the efficiency of PyH photoreactions in the liquid phase of CyH *and in the liquid phases of all of the other media employed here* (*vide infra*) are consistently much lower than in the corresponding solid phases. Much slower rates of solute diffusion and, possibly, the much higher degrees of pyrene

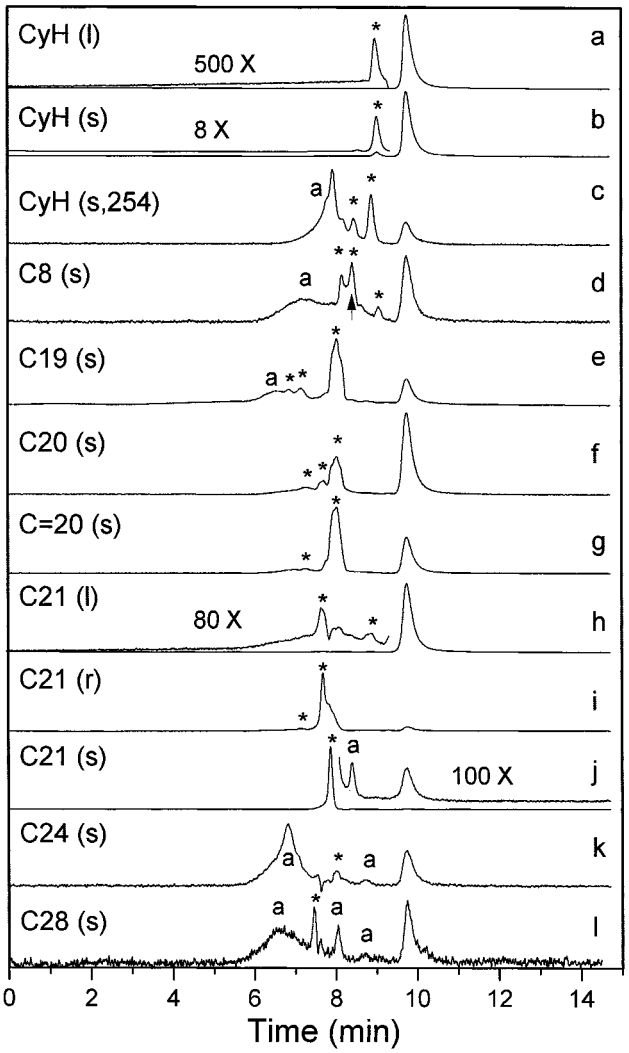

Figure 3. GPC(THF; λ_{det} 343 nm) traces of degassed reaction mixtures after irradiation of degassed sample. Pyrene concentrations and solvents are: ca. 1×10^{-2} M, liquid CyH (a); ca. 1×10^{-2} M, solid CyH (b); ca. 5×10^{-5} M, solid CyH (c); ca. 5×10^{-6} M, solid C8 (d); ca. 5×10^{-6} M, solid C19 (e); ca. 5×10^{-6} M, solid C20 (f); ca. 5×10^{-6} M, solid C=20 (g); ca. 5×10^{-6} M, liquid C21 (h); ca. 5×10^{-6} M, phase I solid C21 (i); ca. 5×10^{-6} M, phase II solid C21 (j); ca. 5×10^{-6} M, solid C24 (k); ca. 5×10^{-6} M, solid C28 (l). Peaks at ca. 10 min correspond to unreacted PyH (and related species). Peaks marked with an "a" are present in the solvent in the absence of PyH; all lack structural absorbances and several are from refraction changes). Peaks marked with an asterisk have UV/vis absorption spectra characteristic of a 1-pyrenyl group. The peak marked with an arrow in (d) has the same retention volume as authentic C8Py. Irradiation conditions: 1 h at >300 nm (a, b, e−l), 2 h at 254 nm (c), 2 h at >310 nm (d). See text for other experimental details.

aggregation in the solid phases account for these observations. Once a highly excited pyrene molecule transfers its energy to a nearby alkane, the two must remain together for a sufficient period to allow a C−H bond of the alkane to be broken and the resulting radical to attach itself to pyrene (Scheme 1). In liquid solutions, cage escape after the initial energy transfer can compete with the subsequent reactive steps.

Irradiations of PyH in C20 and C=20. Irradiations of 10^{-5} M PyH in C20 and C=20 were conducted in their liquid (ca. 45 °C) and solid phases (room temperature) at >300 nm. As noted above, spectral changes were much less evident after irradiation in the liquid than in the solid phase. GPC chromatograms of the solid reaction mixtures demonstrate that several photoadducts had been produced in each case (Figures 3f and 3g). Although several of the peaks in the same retention time regions of the two traces have very similar absorption spectra (such as a 1-alkylpyrene), there are some distinct differences, also. Foremost among these are the peak groups at ca. 7.4 min retention times. The absorption spectra from the C20 mixture are clearly from a simple pyrenyl group; those from the C=20 mixture are not. Although the latter have a vibronic progression in the 300−350 nm region and a sharp peak near 280 nm that are pyrenyl in shape, their positions are red-shifted by ca. 8 nm with respect to those in Figure 3f. Since the only structural difference between the two solvents is at C-1 and C-2, and the mode of PyH incorporation into the solid matrices can be assumed to be the same, either the vinyl groups of C=20 must be near to and react with most of the pyrene molecules or the quantum efficiency for reaction of pyrene molecules near a vinyl group must be much larger than of pyrene in sites with only saturated solvent groups.

Irradiations of PyH in C8, C19, C24, and C28. Irradiation (>310 nm) of 6×10^{-6} M PyH was conducted in the solid (triclinic) phase of C8 for 4 h at −72 °C. Emission spectra after irradiation (not shown) indicated the presence of unreacted PyH and 1-alkylpyrenes. Several photoproducts are evident in the GPC chromatogram of the reaction mixture (Figure 3d). The peak at 9.9 min is unreacted PyH and the one marked with an arrow has the same retention time (and volume) and UV/vis absorption spectrum as commercial C8Py.

The low field regions of the ^{1}H NMR spectra of authentic C8Py and the residue (after removal of C8) from irradiation of 6×10^{-5} M PyH as above but for ca. 60 h are shown in Figure 4. Considering the multiple photoproducts that are present in the reaction mixture, the correspondence between the two spectra is excellent.[60] A singlet at $\delta \cong 3.5$ ppm (in addition to the expected nearby triplet; region not shown in Figure 4a) suggests the presence of more than one species, perhaps from a dihydropyrene such as R−PyH$_2$ in Scheme 1, an impurity from the solvent, or a positional isomer; however, it is difficult to imagine how a positional isomer of C8Py could have a singlet in this region. The photoproduct mixture was also analyzed by GC-MS. The mass spectra of authentic C8Py and the photoproduct peak with the same retention time were indistinguishable except in the molecular ion region (Figure 5). Mass spectra of two other photoproduct peaks in the chromatogram also were indicative of C8Py isomers (N.B., *m*/*e* 215, corresponding to pyrenylmethyene fragments). On these bases, the major photoproduct is 1-octylpyrene (C8Py), and some of the minor photoproducts are its positional isomers (*vide infra*).

Samples of ca. 5×10^{-6} M PyH in C19, C24, and C28 were also irradiated (>300 nm) in their solid phases (20 °C). Emission spectra after irradiation (not shown) indicated the presence of unreacted PyH and 1-alkylpyrenes (Figures 3e, 3k, and 3l). The largest GPC peaks from the C19 reaction mixture (Figure 3e) have UV/vis absorption spectra typical of a 1-pyrenyl chromophore. The large broad peaks and small peaks at ~6.7 min in the GPC traces from irradiations in solid C24 and C28 (marked with an "a") are also present in the GPC traces of "pure" C24 and C28. Their UV/vis spectra consist of unstructured tails with almost no absorbance above 300 nm. Reaction is less efficient in solid C24 or C28 than in solid C19 or C20 (based upon the amounts of unreacted PyH remaining after equivalent radiation times when initial concentrations were the same). However, as in phase II of C21 (*vide infra*), only *one* photoproduct peak, tentatively ascribed to 1-tetracosanylpyrene and 1-octacosanylpyrene, can be detected from the C24 and C28 experiments, respectively. Surprisingly, the perceptible amounts

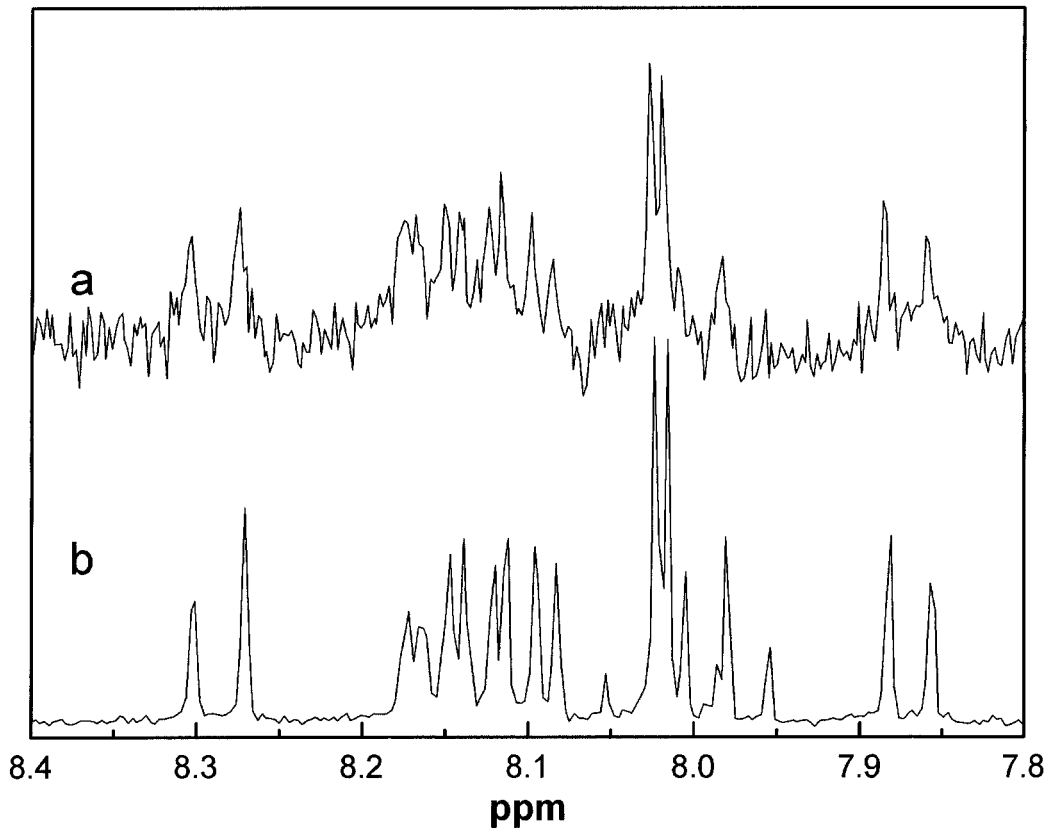

Figure 4. Low field portions of the ^{1}H NMR spectra ($CDCl_3$) of residue (after removal of solvent) from irradiation of ca. 6×10^{-5} M PyH in solid C8 at −72 °C for about 60 h (a) and of authentic C8Py (b). See text.

of solvent impurities do not appear to affect the course of the pyrene photochemistry. It may be too early to generalize that the more ordered solid phases of *all n*-alkanes with ≥ 21 carbon atoms yield only one photoproduct upon irradiation of pyrene since there are only three examples thus far. However, the observation that when $\lambda > 300$ nm, C21, C24, and C28 exhibit much "cleaner" photoreactions with pyrene than do the shorter *n*-alkanes is quite suggestive.

UV Irradiations of PyH in C21. After irradiation (>300 nm) of ca. 5×10^{-6} M PyH in liquid C21 for several hours at 45 °C, no covalent attachment of pyrene or other physical change could be discerned in absorption or emission spectra (not shown), and a GPC trace (Figure 3h) indicated a very small amount of reaction. Although conversion was nearly complete after a similar irradiation of 5×10^{-6} M PyH in the phase I ("rotator") solid of C21 at ca. 35 °C, more than one pyrenyl-containing product was formed (Figure 3i).

Irradiations (>300 nm) of the same concentration of PyH in the phase II (orthorhombic) solid of C21 (slowly or rapidly cooled from the liquid phase to room temperature) led to more rapid formation of *one product* (Figure 3j). We have identified it to be 1-heneicosylpyrene (C21Py) based on the structural evidence that follows.

These results and Figure 2a suggest that pyrene microcrystals or ground-state complexes may participate in the attachment. By contrast, other solid *n*-alkane samples whose emission spectra were primarily from unaggregated PyH molecules could also be converted easily to photoproducts; the presence of aggregates must not be necessary for reaction. However, the course of the photoreactions (and, thereby, the nature of the photoproducts) may be governed by whether isolated or aggregated pyrene is excited initially. Our experiments do not answer this question and it is not addressed in Scheme 1.

In fact, the efficiency of photoreaction in phase II C21 *decreases* with *increasing* PyH concentration for rather subtle reasons. Irradiation of 10^{-2} or 10^{-3} M PyH for up to 50 h gave no discernible reaction, as indicated by front-face emission spectra and GPC analyses. This seemingly anomalous result is probably a consequence of the formation of larger aggregates (perhaps microcrystallites[61]) than those present at the 5×10^{-6} M concentration. Their irradiation could lead to excitonic states[62] whose decay processes deviate from the steps in Scheme 1. Additionally, the fraction of PyH molecules in direct contact with the C21 molecules is diminished significantly as the size of microcrystallites (or other 3-dimensional aggregates) increases; only those PyH molecules on the surface of a microcrystallite have any possibility to reach molecules of C21 and form C21Py.

Irradiations of ca. 5×10^{-6} M PyH in phase II of C21 *at 254 nm* led to several photoproducts (Figure 6). The absorption spectra of all of the photoproduct peaks in the 300−350 nm region have the characteristic vibronic progression of a pyrenyl chromophore. Since irradiations at >300 nm in the same phase and at the same PyH concentration yield only one photoproduct, the mechanisms of the reactions depend on the *absolute energy* of the highly excited triplet Rydberg states involved (Scheme 1).[2−4]

Evidence for the Structure of C21Py. Emission spectra (45 °C; liquid state) of ca. 5×10^{-6} M PyH in C21 before (Figure 2b) and after (Figure 2c) irradiation at room temperature for 1 h are very different. The shapes and positions of bands in Figure 2c are very similar to those of ca. 10^{-5} M C2Py in C21 (Figure 2d).

A GPC chromatogram from the reaction mixture of the rapidly cooled sample is shown in Figure 7a. No additional pyrenyl-containing peaks are detectable at lower attenuations.

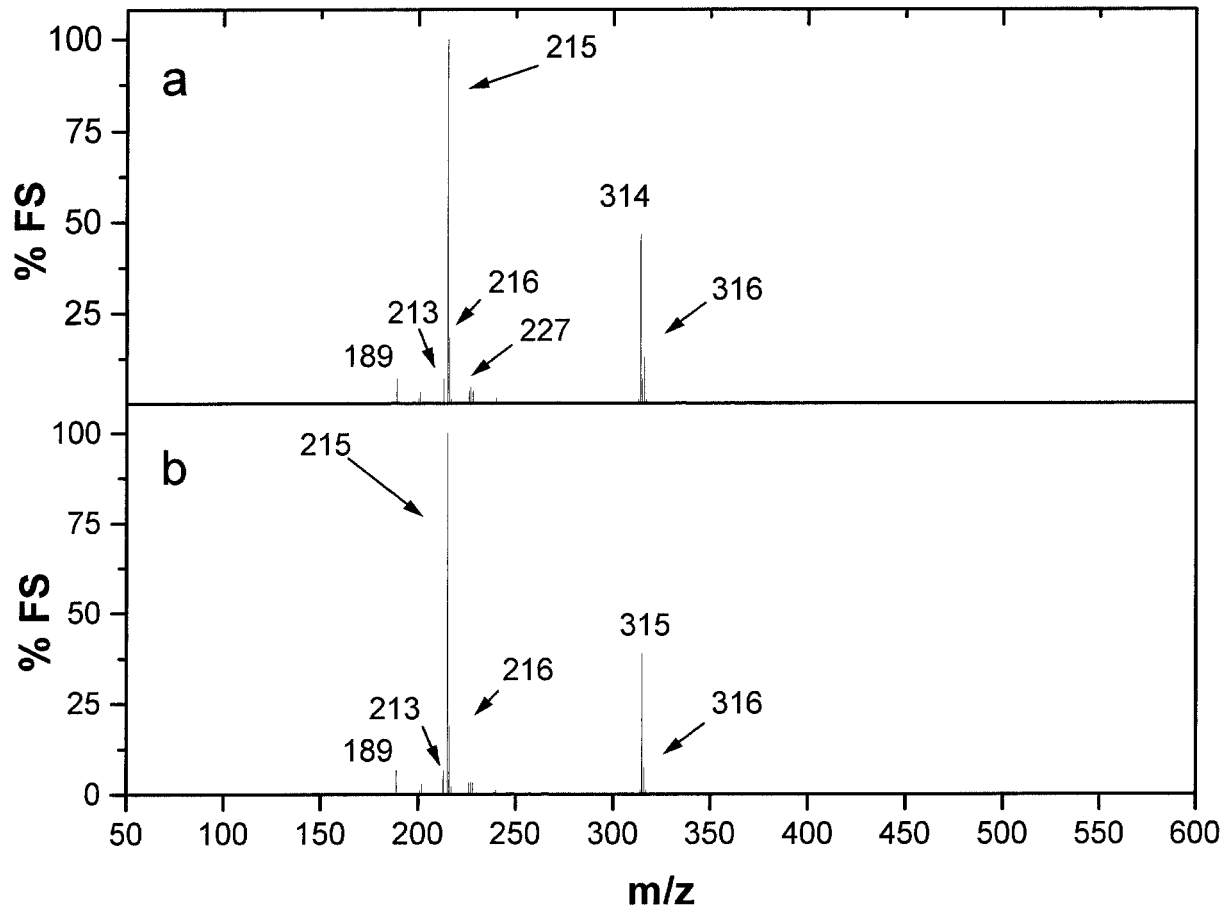

Figure 5. Mass spectra of authentic C8Py (M^+ 314; a) and the reaction mixture from irradiated ca. 6×10^{-5} M PyH in solid C8 (b; see Figure 3). Peaks at *m*/*z* 215 correspond to pyrenylmethylene fragments. The strong *m*/*z* 315 peak in (b) is due to the presence of several products in the sample, including dihydropyrenyl species.

Furthermore, UV absorption spectra at various temporal points along the GPC peak of C21Py (Figure 7b) indicate that there is only one chromophore type, that it is a 1-alkylpyrene in position and shape, and that the peak is homogeneous. Absorption bands in Figure 7b are red-shifted with respect to pyrene by ca. 8 nm; similar shifts are found in absorption spectra of other 1-alkylpyrenes in nonpolar solvents.[33]

We note that the absorption spectra from the GPC peak for residual PyH (Figure 7c) is not homogeneous; before irradiation, it is. The presence of more than one species, each of which must have a molecular mass near that of pyrene, indicates that "side reactions" do occur during irradiations of PyH in phase II of C21, but they do not lead to covalent attachment of solvent to solute. A potential candidate for the other species is dihydropyrene(s), PyH_3 (equation 8 of Scheme 1).[4]

To discern whether the combination of only one molecule of pyrene and C21 leads to C21Py, its retention volume (V_R) and those of several pyrenyl compounds with lower and higher molecular masses and similar structures were compared (Figure 8). The best fit to all of the points has a slight upward curvature. This type of response to mass changes is commonly found when a series of similar compounds is compared.[63] Regardless, the plot and Figure 7b are consistent with C21Py being 1-heneicosylpyrene (rather than a positional isomer of it; *vide infra*). The placement of the data points (open circles) in Figure 8 for the major pyrenyl-containing photoproduct from each of the other solid *n*-alkane irradiations (see Figure 3) is consistent with each of them being an alkylpyrene.

Although higher energy irradiations of pyrene in solid cyclohexane do yield some dicyclohexylpyrene product,[4] there is no direct evidence for attachment of more than one alkane to one pyrene under our experimental conditions. Some of the minor peaks at lower retention times in our GPC traces (N.B., Figures 3e−g) may have multiple attachments. We have observed that irradiation of authentic 1-ethylpyrene in solid C21 is very sluggish; pyrene may be able to add a second alkyl group much less efficiently than the first.

To obtain additional structural evidence for C21Py, a small quantity of it was isolated from the GPC eluant. Its fluorescence spectrum in degassed hexane (Figure 2c) corresponds very closely to that of C2Py (Figure 2e). The differences between the spectra from the reaction mixture (Figure 2d) and the isolated product (Figure 2c) are attributed to emissions in the former from the residual PyH and the other species constituting the GPC peak near 10 min in Figure 3j or 7a. Further evidence for the lumophoric purity of the C21Py comes from its temporal fluorescence decay in hexane (Figure 9). By time-correlated single-photon counting, it could be fitted well to a single exponential function with a decay constant (τ_f) of 247 ± 2 ns. This lifetime is somewhat longer than expected based on τ_f = 192 ns for 1-dodecylpyrene (C12Py) in N_2-saturated cyclohexane,[64] but it is not unreasonable.

The inefficiency of photoreaction at [PyH] ≫ 5×10^{-6} M in solid C21 samples has limited our supply of C21Py. As a result, we have been unable to obtain NMR or mass spectra of the photoproduct. Such data would provide unequivocal evidence for the position of attachment of the 1-pyrenyl group along the heneicosane chain. However, several pieces of ancillary information point to the terminal carbon atom as the sole site of attachment. One of these is the observation that the preferred

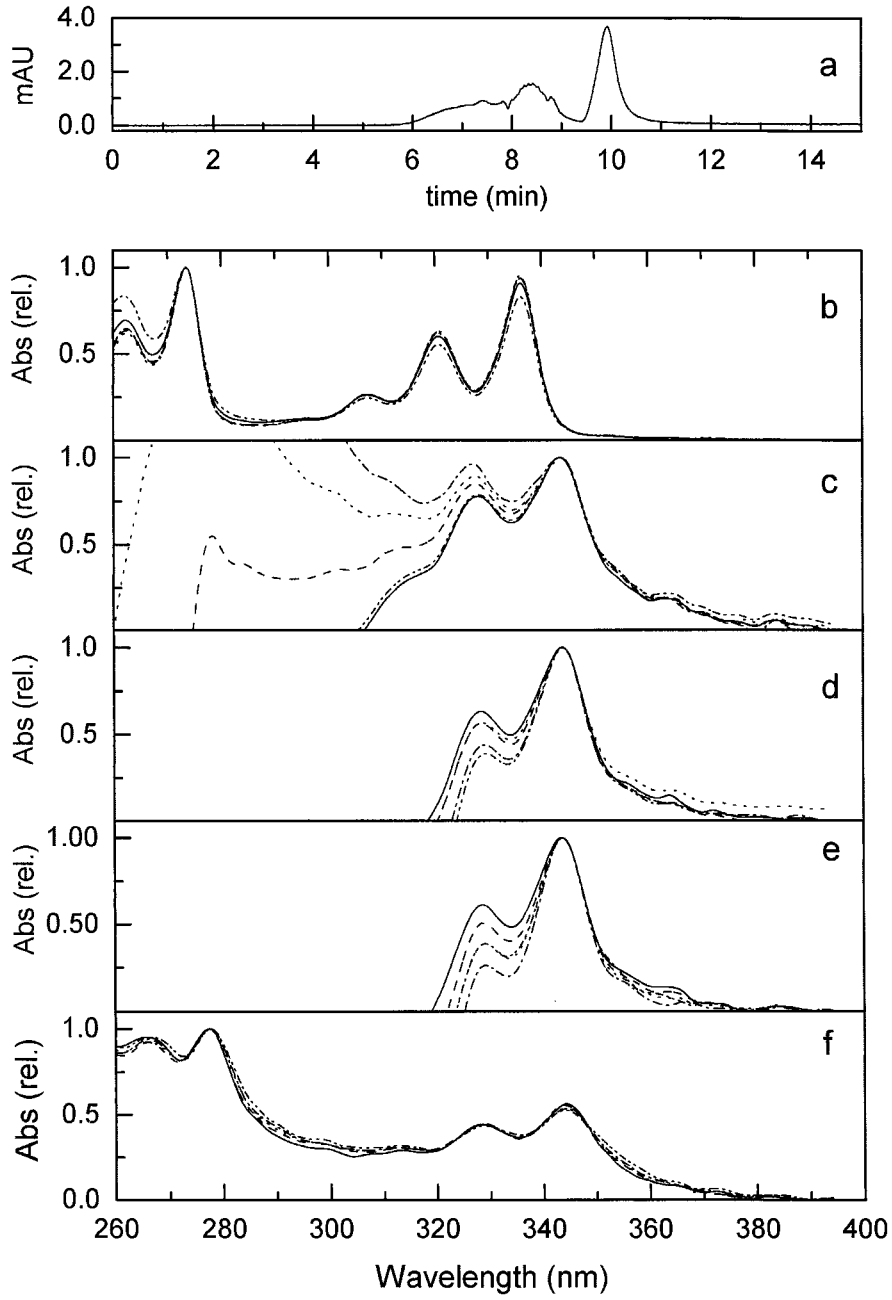

Figure 6. GPC(THF) trace of the reaction mixture from irradiation (254 nm) of ca. 5×10^{-6} M PyH in C21 for 1 h at 20 °C (a; λ_{det} 343 nm). UV/vis absorption spectra from GPC detector corresponding to peaks at ca. 10 min (PyH; b), 9.1 min (c), 8.4 min (d), 7.9 min (e), 7.3 min (f). Overlayed spectra are for slices taken at various points across each peak; each set is normalized internally.

point of attachment of PyH to C8 is at the terminal carbon atom. Another is the similarity of the spectral properties of C21Py and authentic 1-alkylpyrenes. A third is the propensity of *n*-alkanes to form radicals at terminal carbon atoms. γ-Irradiations of *n*-alkanes in SF_6 or as neat solids produce terminal radicals preferentially.[65] This has been shown to be the case for phase II of C21 and the solid phase of C20, as well as other alkanes.[65b]

Conclusions and Future Considerations.

Based on our experimental results, the molecular shapes of PyH and the long *n*-alkanes in their extended conformations, and the expected entropic consequences of placing a pyrene molecule in various locations within a solid *n*-alkane matrix, site **b** in Figure 1 (between layers) is the preferred one. It, alone, provides the steric requirements for preferential attachment by pyrene to terminal carbon atoms of *all* of the solid *n*-alkane matrices. It is also the most different site from that afforded by the plastic or solid phase of cyclohexane (i.e., where multiple photoproducts of attachment are observed). Furthermore, the rather different sets of photoproducts from irradiations of PyH in the phase II (orthorhombic) and phase I (hexagonal) phases of C21 also point to the lamellar boundaries as the contact areas with dopant pyrene molecules. The less rigid rotator phase of C21 is more likely to allow a fraction of the pyrene molecules to reside within a layer and, thereby, form products with a pyrenyl group at different positions along the alkane chain.

Finally, only site **b** explains why the conversion of equal concentrations of pyrene becomes slower as the length of the *n*-alkane host increases. If PyH were preferentially in site **a**, we would expect virtually no rate dependence on the thickness of a host layer. If pyrene is restricted to layer interfaces (site

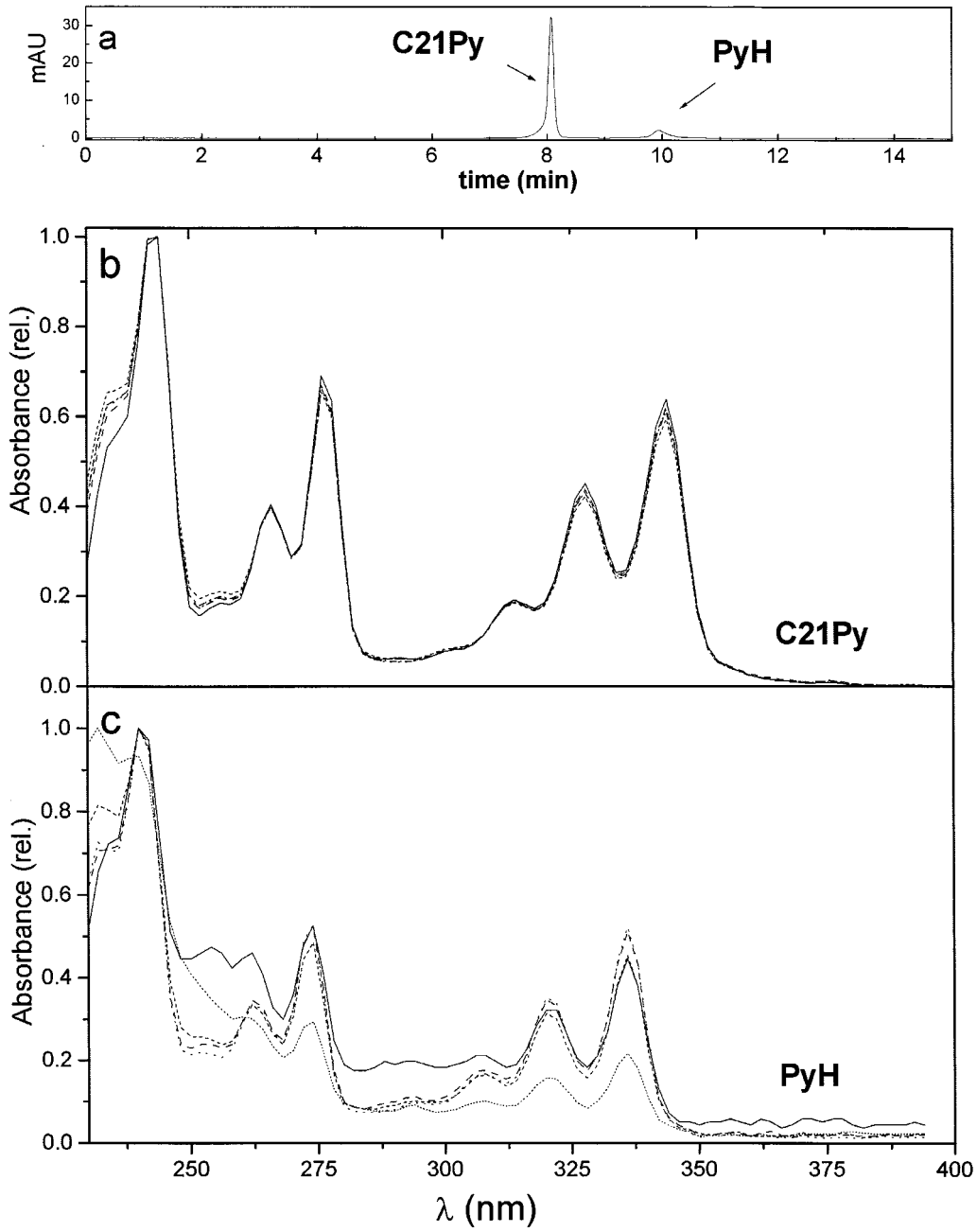

Figure 7. GPC(THF) trace of the reaction mixture from irradiation (> 300 nm) of 5×10^{-6} M PyH in C21 for 1 h at 20 °C (a; λ_{det} 343 nm). UV/vis absorption spectra from GPC detector corresponding to peaks at ca. 8 (C21Py; b) and 10 min (PyH; c). Overlayed spectra are for slices taken at various points across each peak; each set is normalized internally.

b), local PyH concentrations will increase progessively (at a constant bulk concentration) as the alkane length increases; the fraction of the total volume represented by layer interfaces decreases as the thickness of a layer increases. As a consequence, the degree of aggregation and/or size of pyrene aggregates will be greater in solid phases of longer alkanes. As noted before, larger aggregates should lead to less efficient reaction for steric and electronic reasons. However, aggregation must not be due to limited interfacial area. Simple calculations demonstrate that even in the longest *n*-alkane employed, the degree of interfacial coverage by dispersed pyrene (at 5×10^{-6} M) is much less than 1%.

Solutes with more rodlike shapes are known to be incorporated preferentially within an *n*-alkane layer (site **a**).[7,51,66] Recently, it has been shown that a solute molecule in a layered liquid-crystalline phase can be forced by photoinduced shape changes to move reversibly between sites analogous to those in Figure 1.[67] The more rodlike form prefers site **a** and the more platelike form prefers site **b**. The much more viscous environment of solid *n*-alkane matrices forces solutes to decide where they will reside at the moment their host solidifies, and then remain there for periods which are much longer than the duration of a photochemical reaction.

The increased lifetime expected for pyrene triplets when in the solid matrices, due to slower quenching by impurities, makes absorption of a second photon (and reaction from $^3PyH^{**}$) more probable. Lack of mobility in the solid states must contribute also to greater efficiency of photoattachment by keeping alkyl radicals in the vicinity of their pyrene "sensitizer". An alkyl radical is forced to remain in the proximity of its pyrene energy donor by the stiffness of the local environment.[28] At the same time, the preference of the radical center to remain at a terminal

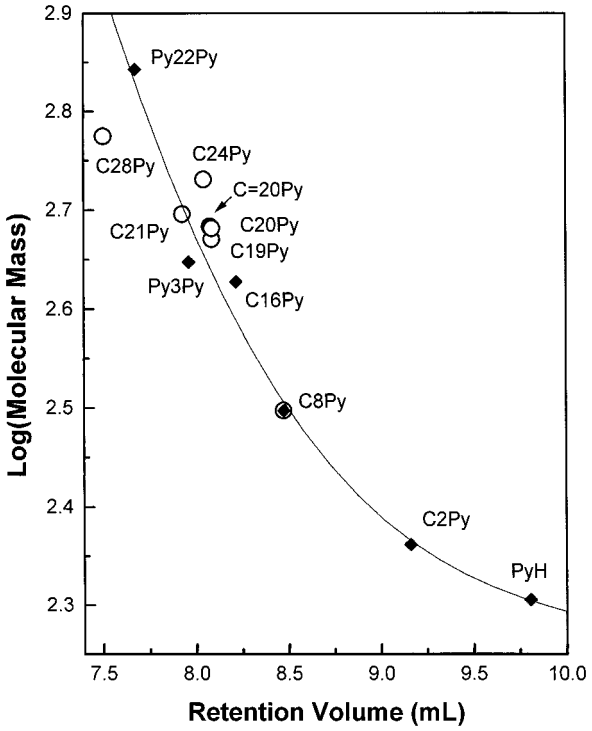

Figure 8. Log (molecular mass) versus retention volumes (V_R) from GPC(THF) traces for a series of authentic 1-pyrenyl derivatives with molecular masses from 202 (PyH) to 696 (Py22Py) (◆) and for the major photoproducts from PyH/*n*-alkane irradiations as shown in Figure 3 (○). The V_R values are an average of at least three measurements. The curve is an empirical best fit to data for authentic samples.

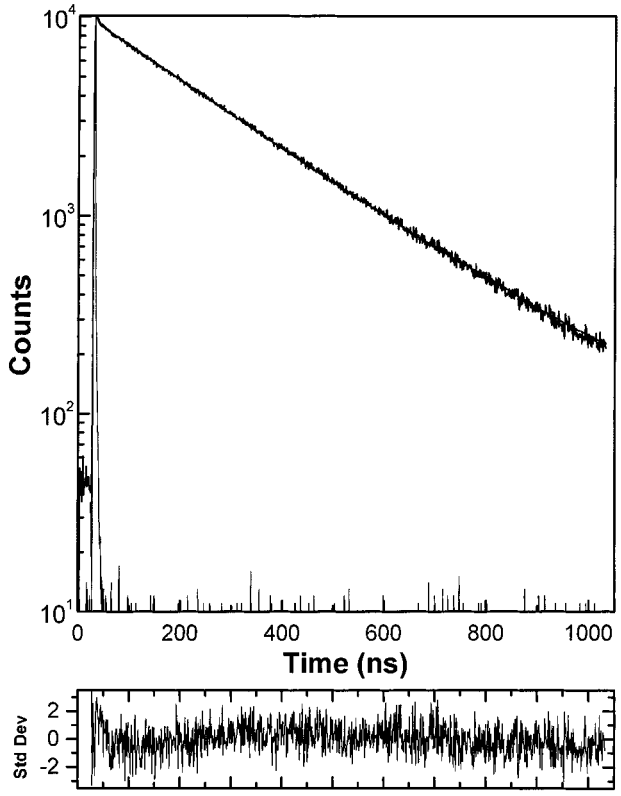

Figure 9. Semilog plot of the time-resolved emission intensity (and residuals to the linear best fit; below) from isolated C21Py in degassed hexane. The lamp pulse profile is included also: λ_{em} 376; λ_{ex} 343 nm.

carbon atom of an *n*-alkane[65] aids the regioselectivity of the highly energetic processes and ensures that the reactive partners will be geminal. We suspect that the high mobility of H·, even in the solid phases, as well as some reversibility of step 8 in Scheme 1, allows the vast majority of photoproducts to be alkylpyrenes rather than dihydropyrenes.

It remains unclear why some solid *n*-alkane matrices provide an environment for "clean" photoattachment while others do not. Although different solvent order and solute mobility may account for why pyrene photochemistry is more selective in the orthorhombic phase II of C21 than in the rotator phase I, these factors do not explain why solid C8 and the other shorter solid *n*-alkane matrices (that are not rotator phases) are less selective. Temperature cannot be the determining factor since pyrene was irradiated in solid C8 at −72 °C and irradiations in phase II of C21 were at 20 °C. The results with C24 and C28, in combination with those from irradiations in C21, suggest that there may be a critical *n*-alkane length beyond which the photoattachment process becomes very selective. Further experimentation with other *n*-alkanes will be required to test this hypothesis.

The wavelength dependence on the photoproduct distributions is rather surprising. It may be related to the relationship between the electronic excitation energy of the Rydberg states of pyrene and its ionization potential. Assuming that excitation to the triplet Rydberg state occurs by absorption of a ≥ 300 nm photon ($E \leq 4.1$ eV) from the lowest vibronic level of T_1 ($E_T = 2.1$ eV;[68] step 3 of Scheme 1), the total energy available for donation to an *n*-alkane by $^3PyH^{**}$ is ≤ 6.2 eV. Thus, the *maximum* energy of excitation provided to $^3PyH^{**}$ is not above the ionization potential of pyrene,[26] but it is adequate to break any of the C−H bonds in pyrene or an *n*-alkane. If excitation from T_1 is via absorption of a 254 nm photon ($E = 4.9$ eV), the total energy available to ^{3}PyH**, 7.0 eV, *exceeds* the ionization potential by 0.8 eV. By maintaining the total energy available to the Rydberg states below the ionization limit, some of the reaction channels followed at higher energies may be avoided. These include processes involving ion radicals.[4]

Overall, these results indicate that several factors must be balanced carefully in order to achieve selective attachment between the terminal carbon of an *n*-alkane and C-1 of pyrene. However, the appropriate conditions *can* be employed using information derived from this work. The next challenge will be to find conditions that maximize the synthetic utility of the reactions. In principle, photoattachment offers a simple, general, one-step route to 1-alkylpyrenes. Even at this point, the small amounts of these probe materials needed for many photophysical studies are available from the irradiation procedures described.

Acknowledgment. We thank the National Science Foundation and the Petroleum Research Fund (administered by the American Chemical Society) for financial support and Prof. René Lapouyade for several very useful suggestions. The authors dedicate this article to the memories of two recently lost colleagues, Professors Juan J. Cosa (Universidad de Río Cuarto, Argentina) and João B. Sargi Bonilha (Universidade de São Paulo at Riberão Preto, Brasil).

References and Notes

(1) Lamotte, M.; Bagno, O.; Lapouyade, R.; Joussot-Dubien, J. *C. R. Acad. Sci., Paris, Serie II*, **1984**, *299*, 1321.

(2) Lamotte, M.; Joussot-Dubien, J.; Lapouyade, R.; Pereyre, J. In *Photophysics and Photochemistry above 6 eV*; Lahmani, F., Ed.; Elsevier: Amsterdam, 1985; 577.

(3) Lamotte, M.; Pereyre, J.; Joussot-Dubien, J.; Lapouyade, R. *J. Photochem.* **1987**, *38*, 177.

(4) Lamotte, M.; Pereyre, J.; Lapouyade, R.; Joussot-Dubien, J. *J. Photochem. Photobiol. A* **1991**, 58, 225.

(5) Naciri, J.; Weiss; R. G. *Macromolecules* **1989**, *22*, 3928.

(6) (a) Wunderlich, B. *Macromolecular Physics*; Academic Press: New York, 1974; Vol. 1. (b) Phillips, P. J. *Chem. Rev.* **1990**, *90*, 425 and references therein. (c) Zimerman, O. E.; Cui, C. X.; Wang, X.; Atvarz, T. D. Z.; Weiss, R. G. *Polymer* **1998**, 39, 1177.

(7) Small, D. M. *The Physical Chemistry of Lipids*, Plenum: New York, 1986; p 103.

(8) Birks, J. K.; Kazzazz, A. A.; King, T. *Proc. R. Soc. (London)* **1966**, *A291*, 556.

(9) Josephy, E.; Radt, F., Eds. *Elsevier's Encyclopedia of Organic Chemistry*; Series III, vol. 14; Elsevier: New York, 1940; p 379.

(10) Anderson, V. C.; Weiss, R. G. *J. Am. Chem. Soc.* **1984**, *106*, 5291.

(11) Perrin, D. D.; Argarego, W. L. F. *Purification of Laboratory Chemicals*, 3rd ed.; Pergamon Press: Exeter, 1988.

(12) Rossini, F. D.; Wagman, D. D.; Evans, W. H.; Levine, S.; Jaffe, I. *Selected Values of Chemical Thermodynamics Properties*. United States Government Printing Office: Washington, D.C., 1952; p 52.

(13) Schaerer, A. A.; Busso, C. J.; Smith, A. E.; Skinner, L. B. *J. Am. Chem. Soc.* **1955**, *77*, 2017.

(14) Sirota, E. B.; Singer, D. M. *J. Chem. Phys.* **1994**, *101*, 10873.

(15) After filtration, the solid was transferred to a beaker, covered with filter paper, left at room-temperature overnight, and dried under vacuum for several hours.

(16) *DMS UV Atlas of Organic Compounds*; Plenum Press: New York, 1966; Vol. III. p E6/T1.

(17) Graselli, J. G.; Ritchey, W. M. *Atlas of Spectral Data and Physical Constants for Organic Compounds*, 2nd ed.; CRC Press: Cleveland, Ohio, 1975; vol. IV, p 369.

(18) Dry ice/ethanol mixture at −72 °C. The transmittance cutoff of the Dewar flask was 310 nm.

(19) (a) Eaton, D. F. *Pure Appl. Chem.* **1990**, *62*, 1631 and references therein. (b) Knutson, J. R.; Beechem, J. M.; Brand, L. *Chem. Phys. Lett.* **1983**, *102*, 501. (c) Beechem, J. M.; Ameloot, M.; Brand, L. *Chem. Phys. Lett.* **1985**, *120*, 466.

(20) See for instance Part III, Chapter 4 in volumes of the series *Photochemistry*; Bryce-Smith, D., Ed.; The Chemical Society: London.

(21) Lamotte, M. *J. Phys. Chem.* **1981**, *85*, 2632.

(22) (a) Lamotte, M.; Lapouyade, R.; Pereyre, J.; Joussot-Dubien, J. *C. R. Acad. Sci., Paris, Serie C* **1980**, *211*, 290. (b) Rima, J.; Lamotte, M.; Joussot-Dubien, J. *Anal. Chem.* **1982**, *54*, 1059.

(23) Lamotte, M.; Lapouyade, R.; Pereyre, J.; Joussot-Dubien, J. *Chem. Commun.* **1980**, 725.

(24) Sun, Y. P.; Ma, B.; Lawson, G. E.; Bunker, C. E.; Rollins, H. W. *Anal. Chim. Acta* **1996**, *319*, 379.

(25) (a) Pandey, S.; Acree, W. E., Jr. *Anal. Chim. Acta* **1997**, *343*, 155. (b) Sun, Y. P.; Ma, B.; Lawson, G. E.; Bunker, C. E.; Rollins, H. W. *Anal. Chim. Acta* **1997**, *343*, 159.

(26) Boschi, R.; Schmit, W. *Tetrahedron Lett.* **1972**, *25*, 2577.

(27) The wave function for the Rydberg electron can be considered independent of the position of individual nuclei. Freund, R. S. In *Rydberg States of Atoms and Molecules*; Stebbings, R. F., Dunning, F. B., Eds.; Cambridge University Press: Cambridge, 1983; chapter 10.

(28) Weiss, R. G.; Ramamurthy, V.; Hammond, G. S. *Acc. Chem. Res.* **1993**, *26*, 530.

(29) (a) Mitchell, R. H.; Lai, Y. H.; Williams, R. V. *J. Org. Chem.* **1979**, *44*, 4733. (b) Lapouyade, R.; Pereyre, J.; Garrigues, P. *C. R. Acad. Sci., Paris, Serie II* **1986**, *10*, 903.

(30) Electronic densities were obtained from ab initio calculations at the HF/6−31 g* level of theory using the *Gaussian 94* program by Frisch, M. J.; Trucks, G. W.; Schlegel, H. B.; Gill, P. M. W.; Johnson, B. G.; Robb, M. A.; Cheesman, J. R.; Keith, T.; Peterson, G. A.; Ortiz, J. V.; Foresman, J. B.; Ciolowski, J.; Stefanov, B. B.; Nanayakkara, A.; Challacombe, M.; Peng, C. Y.; Ayala, P. Y.; Chen, W.; Wong, M. W.; Andre, J. L.; Reploge, E. S.; Gomperts, R.; Martin, R. L.; Fox, D. J.; Binkley, J. S.; Defrees, D. J.; Baker, J.; Stewart, J. P.; Head-Gordon, M.; Gonzalez, C.; Pople, J. A. from Gaussian, Inc. Pittsburgh, PA, 1995.

(31) Joussot-Dubien, J.; Lamotte, M.; Pereyre, J. *J. Photochem.* **1981**, 347.

(32) The authors used a medium-pressure Hg arc lamp with ($\lambda_{ex} > 240$) and without ($\lambda_{ex} > 180$ nm) a Vycor filter.

(33) (a) Naciri, J. Ph.D. Thesis, Georgetown University, Washington, D.C., 1989. (b) Zimerman, O. E.; Weiss, R. G., unpublished results.

(34) Only the rotator phase crystal transition temperature is included. Some *n*-alkanes have more than one distinct rotator phase.

(35) Kitaigorodskii, A. I. *Organic Chemical Crystallography*; Consultants Bureau: New York, 1961, Chapter 4.

(36) Crissman, J. M.; Passaglia, E.; Eby, R. K.; Colson, J. P. *J. Appl. Crystallogr.* **1970**, *3*, 174.

(37) Small, D. M. *The Physical Chemistry of Lipids*; Plenum: New York, 1986, p 103.

(38) Dorset, D. L.; Strauss, H. L.; Snyder, R. G. *J. Phys. Chem.* **1991**, *95*, 938.

(39) Boese, R.; Weiss, H.-C.; Bläser, D. *Angew. Chem., Int. Ed. Engl.* **1999**, *38*, 988.

(40) Kelusky, E. C.; Smith, I. C. P.; Ellinger, C. A.; Cameron, D. G. *J. Am. Chem. Soc.* **1984**, *106*, 2267.

(41) (a) Doucet, J.; Denicolò, I.; Craievich, A. *J. Chem. Phys.* **1981**, *75*, 1523. (b) Denicolo, I.; Doucet, J.; Craievich, A. F. *J. Chem. Phys.* **1983**, *78*, 1465. (c) Maroncelli, M.; Strauss, H. L.; Snyder, R. G. *J. Chem. Phys.* **1985**, *82*, 2811. (d) Okazaki, M.; Toriyama, K. *J. Phys. Chem.* **1989**, *93*, 2883.

(42) Gang, H.; Gang, O.; Shao, H. H.; Wu, X. Z.; Patel, J.; Hsu, C. S.; Deutsch, M.; Ocko, B. M.; Sirota, E. B. *J. Phys. Chem. B* **1998**, *102*, 2754.

(43) Egelstaff, P. A. *J. Chem. Phys.* **1970**, *53*, 2590.

(44) Sherwood, J. N., Ed. *The Plastically Crystalline State: Orientationally Disordered Crystals*; Wiley: New York, 1979; p 29 and refs cited therein.

(45) (a) Thulstrup, E. W.; Eggers, J. H. *Chem. Phys. Lett.* **1968**, *1*, 690. (b) Thulstrup, E. W.; Michl, J.; Eggers, J. H. *J. Phys. Chem.* **1970**, *74*, 3868. (c) Phillips, P. J. *Chem. Rev.* **1990**, *90*, 425.

(46) (a) Naciri, J.; He, Z.; Costantino, R. M.; Lu, L.; Hammond, G. S.; Weiss, R. G. In *Multi-Dimensional NMR, FT-IR/Raman, and Fluorescence Spectroscopy of Polymers*; Urban, M. W., Provder, T., Eds.; American Chemical Society: Washington D.C., 1995; Chapter 25. (b) Cui, C.; Naciri, J.; He, Z.; Jenkins, R. M.; Lu, L.; Ramesh, V.; Hammond, G. S.; Weiss, R. G. *Quimica Nova* **1993**, *16*, 578. (c) Cui, C.; Weiss, R. G. *J. Am. Chem. Soc.* **1993**, *115*, 9820. (d) Talhavini, M.; Atvars, T. D. Z.; Cui, C.; Weiss, R. G. *Polymer* **1996**, *37*, 4365.

(47) Camerman, A.; Trotter, J. *Acta Crystallogr.* **1965**, *18*, 636.

(48) (a) Konwerska-Hrabowska, J. *Appl. Spectrosc.* **1985**, *39*, 434. (b) Konwerska-Hrabowska, J. *Appl. Spectrosc.* **1985**, *39*, 976.

(49) Mathisen, H.; Norman, N.; Pederson, B. F. *Acta Chem. Scand.* **1967**, *21*, 127.

(50) The folded plane is aproximately (001). It is an uneven surface because of the presence of folds, loops, and linking chains. (a) Phillips, P. J. *Chem. Rev.* **1990**, *90*, 425. (b) Hoffman, J. D.; Davis, G. T.; Lauritzen, J. I. In *Treatise on Solid State Chemistry*; Hannay, N. B., Ed.; Plenum Press: New York, 1976; Vol. 3.

(51) (a) Dorset, D. L. *Acta Chim. Hungaria* **1993**, *130*, 389. (b) Clavell-Grunbaum; D.; Strauss, H. L.; Snyder, R. G. *J. Phys. Chem. B* **1997**, *101*, 335.

(52) Kimura, M.; Nukada, K.; Satake, K.; Morosawa, S.; Tampagake, K. *J. Chem. Soc., Perkin Trans. 1* **1984**, 1431.

(53) McGrath, K. J. Ph.D. Thesis, Georgetown University, Washington, D.C., 1994.

(54) Birks, J. B. *Photophysics of Aromatic Molecules*; Wiley: London, 1970; chapter 4.

(55) (a) Birks, J. B. *Photophysics of Aromatic Molecules*; Wiley: London, 1970; p 301. (b) Barltrop, J. A.; Coyle, J. D. *Principles of Photochemistry*; Wiley: Bristol, 1975; p 105.

(56) Yin, G. Z.; Nicol, M. F. *J. Phys. Chem.* **1985**, *89*, 1171.

(57) (a) Bauer, R. K.; Borenstein, R.; de Mayo, P.; Okada, K.; Rafalska, M.; Ware, W. R.; Wu, K. C. *J. Am. Chem. Soc.* **1982**, *104*, 4635. (b) Bauer, R. K.; de Mayo, P.; Okada, K.; Ware, W. R.; Wu, K. C. *J. Phys. Chem.* **1983**, *87*, 460.

(58) Bauer, R. K.; de Mayo, P.; Ware, W. R.; Wu, K. C. *J. Phys. Chem.* **1982**, *86*, 3781.

(59) Excimer-like emissions have been detected by others from 10^{-5} M pyrene in frozen cyclohexane. We do not know whether the protocols for sample preparation were the same as employed here.[59a−c] (a) McDonald, R. J.; Selinger, B. K. *Aust. J. Chem.* **1971**, *24*, 249. (b) Ferguson, J. *J. Chem. Phys.* **1965**, *43*, 306. (c) Mataga, N.; Torihashi, Y.; Ota, Y. *Chem. Phys. Lett.* **1967**, *1*, 385.

(60) (a) Reynders, P.; Kühnle, W.; Zachariasse, K. A. *J. Am. Chem. Soc.* **1990**, *112*, 3929. (b) Reynders, P.; Kühnle, W.; Zachariasse, K. A. *J. Phys. Chem.* **1990**, *94*, 4073.

(61) Avis, P.; Porter, G. *J. Chem Soc.* **1973**, *34*, 1057.

(62) See for instance: Kasha, M.; Rawls, H. R.; El-Bayoumi, M. *Pure Appl. Chem.* **1965**, *11*, 371.

(63) Yau, W. W.; Kirkland, J. J.; Bly, D. D. *Modern Size-Exclusion Liquid Chromatography*; Wiley: New York, 1979.

(64) Jenkins, R. M.; Weiss, R. G. *Langmuir* **1990**, *6*, 1408.

(65) (a) Toriyama, K.; Nunome, K.; Iwasaki, M. *J. Phys. Chem.* **1986**, *90*, 6836. (b) Toriyama, K.; Iwasaki, M.; Nunome, K.; Matsuura, K. *Radiat. Phys. Chem.* **1990**, *37*, 15.

(66) See for instance: (a) Weiss, R. G.; Treanor, R. L.; Nuñez, A. *Pure Appl. Chem.* **1988**, *60*, 999. (b) Nuñez, A.; Hammond, G. S.; Weiss, R. G. *J. Am. Chem. Soc.* **1992**, *114*, 10258.

(67) Lansac, Y.; Glaser, M. A.; Clark, N. A.; Lavrentovich, O. D. *Nature* **1999**, *398*, 54.

(68) Evans, D. F. *J. Chem. Soc.* **1957**, 1351.